

MOE-GEN: High-Throughput MoE Inference on a Single GPU with Module-Based Batching

Tairan Xu^{*1} Leyang Xue^{*1} Zhan Lu¹ Adrian Jackson² Luo Mai¹

Abstract

This paper presents MOE-GEN, a high-throughput MoE inference system optimized for single-GPU execution. Existing inference systems rely on model-based or continuous batching strategies, originally designed for interactive inference, which result in excessively small batches for MoE’s key modules—attention and expert modules—leading to poor throughput. To address this, we introduce module-based batching, which accumulates tokens in host memory and dynamically launches large batches on GPUs to maximize utilization. Additionally, we optimize the choice of batch sizes for each module in an MoE to fully overlap GPU computation and communication, maximizing throughput. Evaluation demonstrates that MOE-GEN achieves 8–31× higher throughput compared to state-of-the-art systems employing model-based batching (FlexGen, MoE-Lightning, DeepSpeed), and offers even greater throughput improvements over continuous batching systems (e.g., vLLM and Ollama) on popular MoE models (DeepSeek and Mixtral) across offline inference tasks. MOE-GEN’s source code is publicly available at <https://github.com/EfficientMoE/MoE-Gen>

1. Introduction

MoE architectures are increasingly favoured in LLMs because their router-based design activates only a subset of experts per token, reducing computational overhead and making them more suitable for deployment on personal machines with limited GPU resources. For locally deployed MoEs, AI developers often run high-throughput inference tasks such as benchmarking (Chiang et al., 2024; Cobbe

^{*}Equal contribution ¹The University of Edinburgh ²EPCC, The University of Edinburgh. Correspondence to: Tairan Xu <t.xu-29@sms.ed.ac.uk>, Leyang Xue <leyang.xue@ed.ac.uk>, Zhan Lu <z.lu-64@sms.ed.ac.uk>, Adrian Jackson <a.jackson@epcc.ed.ac.uk>, Luo Mai <luo.mai@ed.ac.uk>.

	Prefill Expert Avg.			Decoding Expert Avg.		
	Bsz	Util	TP	Bsz	Util	TP
DeepSpeed	153	52%	109	0.3	0.1%	1
FlexGen*	115	49%	77	0.3	0.1%	1
MoE-Lightning*	134	50%	98	0.4	0.1%	1
MOE-GEN	8192	100%	841	75	41%	31

Table 1: Offloading throughput (TP in tokens/s) is measured for *DeepSeek-V2 236B* on an NVIDIA A5000 (24GB) with 512GB of host memory and a context length of 768 tokens (512 for the prompt, 256 for decoding). MOE-GEN’s module-based batching enables up to a 2× increase in GPU FLOPs utilization and a 7.7-11× improvement in throughput. During the decoding phase, MOE-GEN achieves a 31× improvement in throughput. ‘Bsz’ denotes the average number of tokens routed to an expert.

et al., 2021) to evaluate fine-tuned models for personal AI applications, data wrangling (Narayan et al., 2022; van Renen et al., 2024) for cleaning datasets and extracting information, and feature extraction (Mischler et al., 2024; Asai et al., 2023) to generate embeddings for retrieval-based LLMs and other downstream applications. Unlike conventional interactive inference tasks (e.g., ChatBot), high-throughput inference trades off lower latency for higher batch sizes, optimizing overall throughput.

A major challenge for high-throughput MoE inference is the model’s large size, which often exceeds a single GPU’s memory capacity. To overcome this, AI developers use memory offloading, where the full model parameters of an MoE and its KV-cache are stored in host memory—typically much larger and more cost-effective to expand than GPU memory. Parameters and KV-cache are then fetched into the GPU only when activated.

When offloading is enabled, high-throughput LLM inference systems often suffer from low GPU utilization, leading to suboptimal throughput performance. These systems typically use model-based batching, where the entire MoE model processes a batch of input tokens at the model ingress, but within the model, each expert handles only a small fraction of tokens assigned by the router. This results in extremely low GPU utilization during decoding. We illustrate this in Table 1. Systems like FlexGen (Sheng et al., 2023), DeepSpeed-Inference (Aminabadi et al., 2022),

Mixtral-Offloading (Eliseev & Mazur, 2023), and MoE-Lightning (Cao et al., 2024) often operate with batch sizes 40–1000× smaller than what is needed to fully utilize a GPU during LLM decode, significantly reducing throughput compared to the prefill phase. While continuous batching (Yu et al., 2022), as used in interactive inference systems like Llama.cpp (Ollama, 2025) and vLLM (Kwon et al., 2023), could improve GPU utilization, our analysis shows that it is optimized for time-to-first-token (TTFT) rather than throughput. In practice, it leads to even smaller batch sizes during decoding, further lowering throughput.

In this paper, we explore methods to significantly improve high-throughput MoE inference on a single GPU. Our key idea is that MoE models have only two compute-intensive modules: attention and experts. For those two modules, we can accumulate sufficient tokens in the CPU’s host memory to form large batches and ensure that GPUs process them only when the batch size is large enough to fully utilize GPU resources, increasing throughput. Additionally, we carefully optimize batch size so that GPU computation and memory communication are fully overlapped, keeping GPU utilization high. This approach is feasible because CPU memory is significantly cheaper than GPU memory and is typically large enough to store the entire MoE model in an offloading scenario. Moreover, by processing larger batches per module, we reduce the need for repeated host-to-GPU transfers, alleviating I/O bottlenecks. We call this new design module-based batching.

Building on this idea, we design MOE-GEN, a high-throughput MoE inference system that fully utilizes a single GPU. Our key contributions include:

Contribution 1. We propose a module-based batching strategy for MoE architectures, where attention and expert modules are carefully selected and organized to incrementally build large batches, maximizing GPU utilization.

Contribution 2. We propose an optimized system design for high-throughput MoE inference on a single GPU. This design includes full support for module-based batching, enhanced optimizations for managing offloaded KV-cache and model weights, and parallel CPU cores to offload partial computations from the GPU, further improving throughput.

Contribution 3. We formulate an optimization problem to determine the optimal batch size for different attention and expert modules, considering various practical factors such as MoE model architecture (e.g., expert size and count), hardware capabilities (e.g., GPU memory size), and system parameters (e.g., buffer size and peak memory consumption). To solve this, we propose a search policy that efficiently finds the optimized batch size for both prefill and decode phases.

We evaluated MOE-GEN against extensive baseline systems

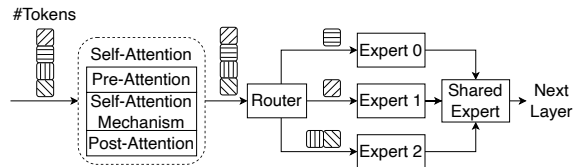


Figure 1: Illustration of one layer in MoE models.

including FlexGen, DeepSpeed-Inference, MoE-Lightening, vLLM and Ollama (llama.cpp) using popular, open-sourced MoE models, including DeepSeek-V2 (DeepSeek-AI et al., 2024) and Mixtral (Jiang et al., 2024a) with benchmarks such as ChatBot-Arena (Chiang et al., 2024), LongBench (Bai et al., 2024), MMLU (Hendrycks et al., 2021) and GSM8K (Cobbe et al., 2021). In the evaluation, MOE-GEN achieves 9-63× less time to complete the inference on datasets with 8K–116K prompts, 16-33× higher decoding throughput across different models on a single commodity GPU compared to model-based offloading systems, and 7.7-11× higher prefill throughput on MoE models with higher sparsity (e.g., DeepSeek). Additionally, MOE-GEN delivers 7-13× throughput improvement for long-context generation (6K–24K context length), fully leveraging the capabilities of state-of-the-art MoE LLMs.

2. Background

MoE inference. We describe the inference process of the MoE model as shown in Figure 1. A typical layer in MoE models consists of a self-attention layer followed by a sparse MoE layer. The input tokens to a layer are first processed by the self-attention layer, which can be generally divided into three stages: the pre-attention stage (e.g., QKV projection), the self-attention mechanism stage (e.g., QK^T), and the post-attention stage (e.g., output projection). After the self-attention layer, tokens are passed to the sparse MoE layer, where a router assigns each token to a subset of experts, typically using a top- k selection strategy. Each token is processed by k selected experts, and the final output is obtained by computing a weighted average of the outputs from these experts. Some model architectures, such as DeepSeek-V2 and Qwen2MoE (Qwen Team, 2024), incorporate a shared expert that all tokens pass through. The processed tokens then proceed to subsequent layers in the model. We omit layer normalization and residual connections in our discussion, as their exclusion does not affect the key structure.

MoE batched inference follows the same procedure as LLM generative inference, which operates in two phases: i) prefill: A batch of prompts is processed to generate the KV-cache at each attention layer. ii) decoding: New tokens are generated in an auto-regressive manner. The output tokens from the previous forward pass are used as the input tokens for generating the next token. In each forward pass, the KV-cache for the new input token is generated and appended to the

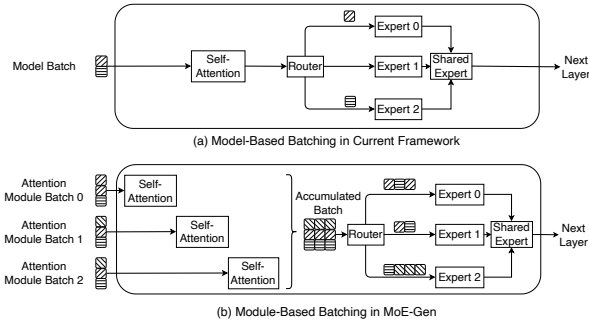


Figure 2: Model-based batching employs a single, unified batch size throughout the entire forward pass, whereas module-based batching iteratively process modules with small batches to form larger batches.

existing KV-cache, forming the complete context so far. The computational intensity in the decoding phase is typically orders of magnitude lower than in the prefilling phase, as only one token per sequence is passed into the model.

MoE offloading. The offloading system typically manages two levels of memory: CPU memory for excess model weights and key-value (KV) states, and GPU memory for computation and fast data access. When model weights are required for GPU computation, they can either be fetched in advance (overlapped with other computations) or fetched on-demand. A resident store can be designed in GPU memory to persistently hold model weights and/or KV-cache, while a staging *buffer* is used to prefetch dynamic data. If the GPU attempts to compute with data (e.g., weights or KV states) that are not yet in its resident store, it must stall until the data are transferred from CPU memory.

In offloading systems, the bandwidth between the host and memory is often a scarce resource. Leveraging CPU computation resources to process data locally can potentially increase overall throughput (Cao et al., 2024).

3. Related Work

We show the commonly applied model-based batching and MOE-GEN’s module-based batching in Figure 2. **(1) Model-based batching.** DeepSpeed-Inference (Aminabadi et al., 2022) and FlexGen (Sheng et al., 2023) are designed for dense transformer models and treat MoE layers as dense MLP layers, resulting in insufficient batch sizes for expert layers. FlexGen processes multiple rounds of forward passes reusing the same fetched model weights. In each forward pass, a unified batch is propagated through the entire model, without addressing the batch size limitation for MoE experts. MoE-Lightning (Cao et al., 2024) improves performance over FlexGen by optimizing GPU-CPU-I/O overlap but retains the same batching strategy. Mixtral Offloading (Eliseev & Mazur, 2023) supports the offloading of Mixtral-series of MoE models, making them popular among users with

limited GPU resources.

(2) Continuous batching for high throughput. Continuous batching is orthogonal to both model-based and module-based batching, as it operates at the sequence level. Each forward pass still relies on model-based batching.

Continuous batching frameworks often insert small prefill batches (frequently of size 1) into the decoding phase, leading to an even smaller average batch size over the entire execution.

Frameworks supporting continuous batching include vLLM (Kwon et al., 2023), TensorRT-LLM (NVIDIA, 2024), and Llama.cpp (Ollama, 2025). NEO (Jiang et al., 2024b) interleaves prefill and decoding across the GPU and CPU, while systems such as BlendServe (Zhao et al., 2024) and others (Luan et al., 2024) share the GPU in the temporal domain using micro-batches—ultimately facing the same issue as vLLM. In offloading scenarios, continuous batching performs even worse than traditional model-based batching. Therefore, we exclude it from further discussion in this paper and only report the result for reference.

(3) Batching in training systems. Training systems often interoperate fixed global batch sizes to ensure accuracy. They seek to reduce communication overhead between GPUs over bottlenecked links (Liu et al., 2023; Li et al., 2023; Zhai et al., 2023). This is orthogonal to inference systems where batch size can vary without affecting the model quality. Training systems only have prefilling (Zheng et al., 2022), while decoding is not the major concern.

(4) Interactive inference systems with offloading. Pregate-MoE (Hwang et al., 2024), ExpertFlow (He et al., 2024), MoE-Infinity (Xue et al., 2024), ProMoE (Song et al., 2024) and BrainStorm (Cui et al., 2023) use predictors to instruct expert prefetching before batched inference. While experts are often densely activated under large batch sizes, the prediction-based optimization becomes unnecessary for throughput optimizations. Fiddler (Kamahori et al., 2024) and PowerInfer (Song et al., 2023) support running attention or experts on CPU to alleviate the I/O bottleneck, while mainly optimized for latency in small batch sizes. EdgeMoE (Yi et al., 2023), AdapMoE (Zhong et al., 2024), and Hobbit (Tangl et al., 2024) reduce I/O traffic by replacing high-precision expert parameters with quantized versions. These methods may incur accuracy loss as sparsity increases (Harma et al., 2024).

4. Module-Based Batching

4.1. Design Intuition

We aim to design a batching engine and strategy that accomplish two key objectives: (i) ensuring sufficient large input batches for modules to fully utilize GPU FLOPs, and (ii)

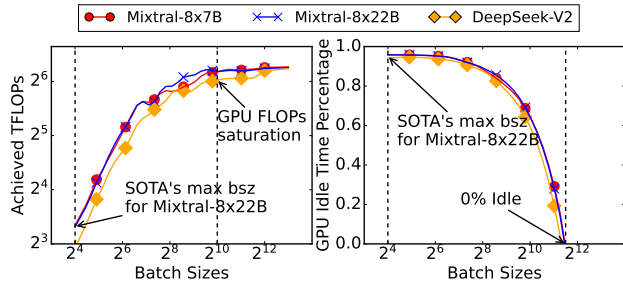


Figure 3: Left: Achieved FLOPs in the non-offloading scenario. This metric represents the number of floating-point operations performed by an expert module, normalized by the GPU compute time. Right: Percentage of GPU idle time in the offloading scenario on an NVIDIA A5000 (PCIe 4.0, 32 GB/s). This metric measures the ratio of the expert module’s execution time to the time required to transfer the necessary weights from the CPU to the GPU.

overlapping computation and fetching times to reduce the end-to-end execution time.

Necessity of large batch size. We make a key observation: the batch size for model-based batching is constrained by the module with the highest memory usage—often the attention module. However, because each expert has low arithmetic intensity, a substantially larger batch size is required to achieve optimal GPU utilization.

As shown in Figure 3 (Left), at least 2^{10} tokens are required to fully utilize GPU compute, whereas the average number of input tokens per expert in current SOTA models is only 2^4 . Furthermore, in Figure 3 (Right), we illustrate a common scenario in offloading: the computation of an expert should be fully overlapped with the fetching of the next expert, resulting in zero GPU idle time. In this case, more than 2^{11} input tokens per expert are needed to ensure that the GPU does not remain idle while waiting for memory transfers. Thus, aggregating a larger batch size for experts is essential to achieve optimal performance. Similar phenomenon has also been observed in the forward pass of attention module in the decoding phase.

Necessity of searching batching strategy. While our main goal is to improve device utilization by increasing input batch sizes for modules, other factors can also affect the execution time of a forward pass. Their influence on throughput is primarily indirect, operating through the utilization or conservation of resources (e.g., GPU memory, PCIe bandwidth). For example, applying CPU-based computation to tasks that remain in host memory can save scarce HtoD memory bandwidth. However, whether this saving translates into throughput gains depends on (1) the CPU’s computation speed and (2) whether we have reserved sufficient GPU buffer to effectively leverage the saved bandwidth. Similarly, if a module requires complex memory reshaping or migration, it may introduce delays but can also provide opportunities to over-

lap memory copy operations. Appropriate configurations must be chosen to seize this opportunity. Consequently, a searching strategy is necessary to determine the resulting throughput and select the optimal configurations.

Means to facilitate large batch size. We need to ensure that the GPU memory is sufficient to process large amounts of input in a single module. During module execution, design-dependent intermediate states (e.g., QKV projections in standard attention or the up-projection result of compressed KV-cache in DeepSeek) can consume significant GPU memory at runtime, which constrains the achievable batch size. To address this, MOE-GEN aims to keep fewer model weights and less KV-cache data on the GPU, thereby facilitating the use of larger batch sizes.

4.2. MOE-GEN Engine Design

Module-based batching. We propose the batching strategy of MOE-GEN as shown in Figure 2. As we observe different modules have distinct memory and FLOP requirements, MOE-GEN instead assigns different batch sizes to each module, i.e., attention and expert. We choose these two components as the base for batching, since the attention module present higher memory demand, which is suitable for lower batch size. Conversely, the expert needs to scale to larger batch size, presenting two extremes. MOE-GEN then accumulates multiple attention batches and processes them in one at the expert module stage, effectively increasing the batch size for the expert module.

Sequential execution of experts. Under large batch sizes, the number of tokens routed to each expert is often uniformly distributed, as observed in previous work and by design of the MoE auxiliary loss (Xue et al., 2024; Jiang et al., 2024a). Consequently, MOE-GEN does not rely on heuristics or prediction-based prefetching. Instead, it focuses on enabling large batch sizes and prefetching, executing experts in a sparse MoE layer sequentially.

Full KV-cache offloading. We initially consider KV-cache partial offloading (Kwon et al., 2023). However, we demonstrate that fully offloading the KV-cache outperforms partial offloading, particularly when considering the completion time for processing an entire dataset. The primary reason is that caching the KV-cache in GPU memory limits batch size, leading to increased fetching traffic for expert weights (e.g., up to 86GB for Mixtral-8x7B). By trading off KV-cache copying, MOE-GEN achieves up to 20× savings in fetching traffic, as shown in Figure 4. While smaller datasets may benefit from retaining KV-cache in GPU memory, especially as GPU memory capacity increases (shown in Figure 4 (b)), popular benchmarking datasets are typically orders of magnitude larger, making KV-cache offloading more advantageous.

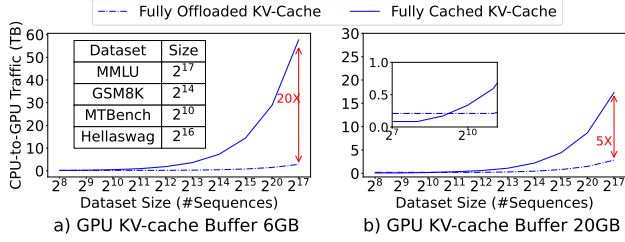


Figure 4: Fetching traffic over dataset, showing fully offloaded KV-cache benefits performance. Using Mixtral-8x7B with CPU KV-cache capacity 128GB. We pad/truncate each prompt to same length and decode same length.

Single GPU buffer for dense modules. In MoE models, in contrast to sparse activated experts, there are dense modules that would be activated for each token (e.g., attention modules and shared experts in DeepSeek). We find that setting the GPU prefetch buffer size to the size of dense modules in a single layer is sufficient to create overlapping. The fetching of such modules only has two cases: (i) *with sufficient HtoD bandwidth*: dense modules can be prefetched and fully overlapped; (ii) *without sufficient HtoD bandwidth*: as bandwidth is fully occupied by expert fetching, dense modules need to be fetched on demand. In both cases, the buffer can be cleared and repurposed to the next dense module. Empirically, we verified that assigning more buffer space to dense modules would not increase throughput. When they are large, they could downgrade performance by squeezing the space for other components.

CPU for self-attention. Matrix multiplications on the CPU (e.g., attention projection and expert) are often 10-100x slower than computation on the GPU even accounting for the fetching time of weights (NVIDIA, 2025; Kamahori et al., 2024). Due to the arithmetic intensity in matrix-vector multiplications (GEMV) in QK^T operation, CPU can process data at a pace comparable to the time required to transfer data with PCIe4.0 to the GPU and perform computations there. (Song et al., 2023; Cao et al., 2024). We only use the CPU to compute self-attention mechanism in MOE-GEN. This requires a custom CPU kernel to be implemented with better cache performance than current PyTorch and CBLAS, similar to the CPU version of FlashAttention (Dao, 2024).

System components. Our design choices has led to the system architecture shown in Figure 5. MOE-GEN features a batching scheduler, creating batching strategy based on hardware (e.g., connection speed, GPU memory capacity) and software (e.g., performance and memory usage of GPU and CPU kernels under various input batch sizes) profiling. Using this information, the scheduler enumerates candidate configurations in the search space and applies them to the DAG constructor to estimate the overall runtime of each configuration. It then selects the configuration with the shortest completion time and sends its decision to the MOE-GEN Engine, which is responsible for executing the inference. At

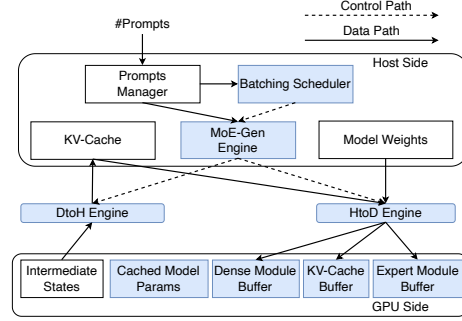


Figure 5: MOE-GEN system components.

this point, the KV-cache buffer, expert module buffer, and dense module buffer are allocated in GPU memory based on the selected configuration’s size requirements.

The MOE-GEN Engine launches batched module execution and submits batched memory copy tasks to the HtoD engine in advance. The engine accumulates batches at each attention layer and MoE layer. Meanwhile, KV-cache offloading and update tasks are submitted to the DtoH engine at runtime. The MOE-GEN Engine also manages all necessary synchronization between computation and memory-copy operations. Details about workload profiling and implementation of the engine are in Appendix B.

4.3. Batching Strategy Formulation

Problem Formulation. The batching strategy is working under the following hardware settings. We consider a machine with two devices: a GPU and a CPU, both of which have memory capacity and computational capabilities. The two levels of memory hierarchy are interconnected with two links HtoD link and DtoH link, which only does data transmission. As the MoE model and corresponding KV-cache cannot fit entirely within the GPU, we offload them to Host memory that is close to the CPU.

Our aim is to find the module-based batching strategy that leads to the maximum throughput under the given system capability. Equivalently, we look for an accumulated batch size B constrained by the memory capacity and corresponding minimal runtime T of the batch. This includes managing micro-batches for each module separately and scheduling computation and memory copies.

Search Space. Given the formulation above, we construct a search space for possible system hyperparameters that affect the execution time T given accumulated batch size B (shown in Equation (1)). The time is a function of components as in Section 2. The variables in the search space that would influence the throughput are shown in Table 2.

$$\underset{B, b_a, b_e, \omega, S_{\text{expert}}, S_{\text{Params}}}{\text{maximize}} \quad \frac{B}{T(B, S_{\text{Expert}}, S_{\text{Params}}, b_a, b_e, \omega)} \quad (1)$$

This search space is constrained by host memory capacity

Notations	Meaning
<i>System & Model Parameters (Profiled)</i>	
m_c	Host memory capacity
m_g	GPU memory capacity
S_{Model}	Size of the model
<i>Functions</i>	
$S_{\text{KV-CPU}}$	Size of KV cache in CPU memory.
$S_{\text{KV-GPU}}$	Size of KV cache in GPU memory.
T	Execution time for a batch B
S_{IS}	Size of intermediate states in execution
<i>Constants (Predetermined)</i>	
S_{Dense}	GPU prefetch buffer size for dense modules
<i>Variables</i>	
B	Accumulated batch size for sparse MoE layer
b_a	GPU attention module batch size
b_e	GPU expert module batch size
ω	Split ratio of B to CPU for attention module
S_{Expert}	Reserved GPU buffer size for expert modules
S_{Params}	Size of cached model parameters in the GPU

Table 2: Notations for the search space.

and GPU memory capacity as in Equations (2) and (3)

$$S_{\text{KV-CPU}}(B) + S_{\text{Model}} \leq m_c \quad (2)$$

$$S_{\text{Params}} + S_{\text{Expert}} + S_{\text{Dense}} + S_{\text{KV-GPU}}(b_a) + S_{\text{IS}}(B, b_a, b_e) \leq m_g \quad (3)$$

We consider the following factors in the search space:

P-D disaggregation. A widely adopted approach, known as the prefill-decode (P-D) disaggregation (Patel et al., 2024; Kwon et al., 2023), defines two classes of DAGs. During the prefill phase, there is no HtoD KV-cache copy in the DAG, whereas the decoding phase considers all possible nodes, as shown in Figure 6. The parameter B has minimal effect on S_{IS} during decoding, since the hidden states it influences is typically sized in MBs, thus incurring negligible overheads. Consequently, we set B in the decoding phase to the maximum value permitted by the host memory size.

Module micro-batch size b_a and b_e . Choosing b_a presents a tradeoff between two types of overhead: (i) the traffic on HtoD link due to insufficient cached model weights with larger b_a , and (ii) GPU underutilization due to attention kernel launch with smaller b_a . Larger b_a uses more space for intermediate states in the GPU, squeezing the space for expert buffer, KV-cache buffer and cached model parameters. Smaller b_a reduces arithmetic intensity, risking underutilization of GPU computations as shown in Section 2.

Similar consideration applies to the selection of b_e . Furthermore, while we estimate the number of tokens routed to each expert by assuming an even distribution, the actual number remains unknown until runtime. Therefore, b_e is chosen to prevent out-of-memory (OOM) errors.

Accumulated batch split ratio to CPU ω . Choosing the split ratio considers the following factors: (i) CPU computa-

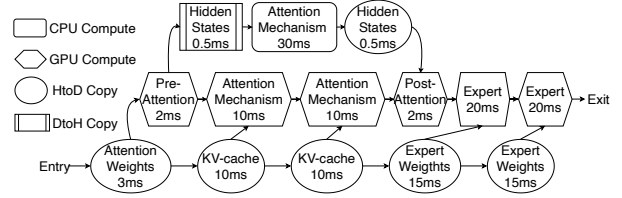


Figure 6: MoE offloading DAG for module-based batching. The dependencies are denoted with arrows.

tion latency *Self Attn*, comparing to (ii) HtoD copy overhead of the KV-cache together with GPU computation latency and (iii) bandwidth for expert prefetching. CPU-based computation reduces the HtoD overhead and its bandwidth usage as the KV-cache stays in Host memory. CPU does not need to finish at the same time or earlier as GPU as in conventional load balanced scheduling, bandwidth saving for prefetching large amount of expert can be better.

Size of reserved GPU buffer S_{Expert} . We aim to select an appropriate size that allows the HtoD engine to prefetch expert weights into the GPU whenever there are periods of idle PCIe time, without overly consuming scarce GPU memory.

Size of cached model parameters in GPU S_{Params} . It is possible that the entire process is memory-bound, so adding S_{Expert} or b_a may not yield any benefit. In this case, using the spare GPU space to cache part of the model parameters reduces HtoD traffic for copying model weights, thereby alleviating memory-bound constraints.

4.4. Searching Batching Strategy

MoE offloading as a DAG. We can view the model inference as a Directed Acyclic Graph (DAG) of jobs. The edges of the DAG represent job dependencies, and each node has the following attributes: i) job execution time, being determined by model, hardware platform and context length, ii) type of the job, being either computation or memory copy. Figure 6 shows such an example, with the assumption that CPU and GPU run the attention module in parallel followed by memory copy and execution of the expert module.

In the decoding phase, the processing starts by copying attention module weights (if offloaded) to GPU memory. Then the GPU computation for the attention mechanism depends on the results from *Pre-Attention* and corresponding *KV-cache* copy. Meanwhile, the CPU kernel for attention mechanism would launch and only depends on *Pre-Attention* results because the KV-cache are fully offloaded to host memory and CPU kernel can access it directly. After batches of attention mechanism are completed, the results from both CPU and GPU are concatenated and pass through the *Post-Attention* stage. In the followed sparse MoE layer, experts are sequentially executed dependent on the copy of their module weights. and GPU computation for self-attention

Config.	GPU	CPU	Host Memory
C1	A5000 24GB	AMD 7453 28-Core	256GB
C2	A5000 24GB	AMD 7453 28-Core	512GB
C3	A6000 48GB	AMD 7313P 16-Core	480GB

Table 3: Testbed configurations.

mechanism depends on the results of Pre-Attention.

Solving minimal runtime on DAG. With DAG, we abstract the problem of estimating the time consumption of inference to Dynamic Programming for the Longest Path (Critical Path). Let $dp[v]$ represent the earliest finishing time of node v in the DAG. Initialize $dp[v] = 0$ for all nodes v except the entry node. The $dp[entry]$ is set to the time cost of itself. Traverse the nodes in topological order, for each node v :

$$dp[v] = \max_{u \in \text{predecessors}(v)} (dp[u]) + \text{cost}(v). \quad (4)$$

The $dp[exit]$ represents the finishing time for this DAG.

5. Evaluation

5.1. Experiments Setup

Hardware. We conduct benchmarks on various hardware settings as shown in Table 3. We aim to benchmark the system performance under various memory capacity, GPU and CPU computational power. C3 has more powerful GPU and larger GPU memory comparing to C1 C2 and C3, while the CPU is weaker.

Datasets. We used a large variety of LLM tasks that covers long prompting (for prefilling performance) or long output tokens (for decoding performance), including LongBench (Bai et al., 2024) for long context generation, MMLU (Hendrycks et al., 2021) for multiple choice questions, aiming for prefilling and GSM8K (Cobbe et al., 2021) for math problems and Chatbot-Arena (Chiang et al., 2024) for multi-round chat.

Models. We include popular open-sourced MoE models in our evaluations including Mixtral-8x7B, Mixtral-8x22B, DeepSeekV2-236B and DeepSeekR1-671B. We exclude text-to-text generation models such as NLLB-MoE (Costa-jussà et al., 2022), as the output length has less variation in response to the input prompt length. OLMoE (Muennighoff et al., 2024) and Phi (Abdin et al., 2024) do not require offloading, thus are omitted in the experiment.

Baselines. We evaluate MOE-GEN and MOE-GEN’s variant for breakdown, comparing them against baseline systems that support running LLMs with offloading: (i) **Llama.cpp** and **vLLM** which support continuous batching; (ii) **DeepSpeed**, **FlexGen*** and **MoE-Lightning*** which support model-based batching; FlexGen does not support MoE models and MoE-Lightning has not yet open sourced, so we replicate their performance using our own imple-

→Num. Sequences (Prompt Len, Decoding Len)	MMLU 116K (512,1)	GSM8K 8.5K (512,256)	ChatBotArena 36K (256,512)
Llama.cpp	149hr	374hr	6423hr
vLLM	112hr	303hr	5205hr
DeepSpeed	23hr	115hr	1710hr
FlexGen*	25hr	122hr	5132hr
MoE-Lightning*	23hr	68hr	5123hr
MOE-GEN(G)	18hr	12hr	124hr
MOE-GEN(H)	18hr	8hr	82hr

Table 4: Time to complete dataset on C2 with Mixtral-8x22B, including model loading time.

mentation. We choose the inference-specific version of DeepSpeed as the baseline. Mixtral-Offloading only supports the Mixtral model and has inferior performance than DeepSpeed, thus we omit it from evaluation.

The baselines are compared with two versions of MOE-GEN: (i) **MOE-GEN(G)** which only uses GPU for all computation, and (ii) **MOE-GEN(H)** which incorporates the CPU attention for expert offloading bandwidth savings. MOE-GEN (G) aligns with most baselines that all computations are performed in GPU, except for Llama.cpp, FlexGen and MoE-Lightning, which align with MOE-GEN (H).

All baseline (vLLM, Llama.cpp, MoE-Lightning) and versions of MOE-GEN using requests padded to the maximum prompt length and with continuous batching disabled (when possible), as aligned with FlexGen.

5.2. End-to-end Performance

Time to complete a dataset. We evaluate the total time for MOE-GEN and the baselines to complete offline inference on large datasets. Note that MMLU only has a prefilling phase, where the first tokens are used as the answer. Table 4 reports the performance. For runtime larger than 24hr, we estimate the overall time using partial dataset.

Mixtral-8x22B is relatively dense, given its “top-2 from 8” expert routing policy. Under traditional model-based batching, with an input prompt length of 512 and a small batch size of 16, each expert is routed 2^{11} tokens in the prefill phase, reaching the saturation region (see Figure 3). Therefore, on prefilling-only task like MMLU, MOE-GEN provides smaller gains(1.3-1.4 \times) compared to decoding tasks such as the rest three datasets. For a much sparser model like DeepSeek-V2 (with a “top-6 from 160” expert routing policy), the performance of baselines during prefilling degrades dramatically, as shown in Table 7.

In the decoding phase, model-based batching yields a low computation workload per expert. Therefore, MOE-GEN (H) significantly outperforms the baselines. On GSM8K, MOE-GEN (H) achieves a 9–15 \times speedup, and when the decoding length is doubled in ChatbotArena, MOE-GEN (H) improves by 21–63 \times . The performance difference be-

Throughput	Config.	Power	Cost
140	8xNVIDIA-A5000	1600W	20K\$
	1xAMD-7453	100W	1.2K\$
	512GB Host	80W	1.1K\$
vLLM		1780W	22.3K\$
143	1xNVIDIA-A5000	200W	2.5K\$
	1xAMD-7453	100W	1.2K\$
	512GB Host	80W	1.1K\$
MOE-GEN		380W	4.8K\$

Table 5: Server settings to save cost. Mixtral-8x22B.

→Models	Mixtral 8x7B		Mixtral 8x22B		DeepSeek-V2 236B		DeepSeek-R1 671B	
→Decode Len	256	1024	256	1024	256	1024	256	1024
Llama.cpp	4	3	2	0.8	1	0.3	0.9	<0.1
vLLM	31	14	2	1	0.8	<0.1	Fail	Fail
DeepSpeed	27	26	4	3	1	1	Fail	Fail
FlexGen*	33	30	5	4	1	1	Fail	Fail
MoE-Lightning*	89	78	9	6	1	1	Fail	Fail
MOE-GEN(G)	195	93	54	27	31	16	17	9
MOE-GEN(H)	469	283	91	57	31	16	17	9

Table 6: Decoding throughput (token/s) on C2 with prompt length 512.

tween MOE-GEN (G) and MOE-GEN (H) underscores the effectiveness of our engine in leveraging CPU computation.

Cost savings. We demonstrate that MOE-GEN enables cost savings by exchanging GPU costs and power with host memory utilization. MOE-GEN supports models with hundreds of GB in size and thousands in batch size on a single GPU workstation. Previously, users needed to invest in expensive and power-hungry 8-GPU servers. Table 5 presents the results. Instead of investing in powerful 8-GPU servers and underutilizing host memory, the same workload can be deployed across eight memory-enhanced servers, each equipped with a single GPU.

As shown in Table 5, MOE-GEN achieves a comparable throughput of an 8-GPU server with a single GPU, while requiring only 21% of the infrastructure budget and corresponding power. The host memory’s low power consumption is the key to the efficiency (in (Fu et al., 2024)). This configuration also achieves comparable throughput.

5.3. MOE-GEN Breakdown

Decoding throughput. We evaluate the total decoding throughput under an increasing KV-cache size throughout the decoding process. Table 6 presents the results. Overall, MOE-GEN achieves a 16-31× throughput improvement over the baselines, showing more pronounced gains for models with higher sparsity, such as DeepSeek. Note that, for DeepSeek, the latent KV-cache must be up-projected by a factor of 71 at runtime. Performing this projection on the CPU or copying the projected results from the device to the host (DtoH) introduces substantial overhead. Consequently, for DeepSeek-V2, the split ratio w is set to zero, which aligns with the configuration used by MOE-GEN (G).

Prefill throughput. Table 7 reports the performance. MOE-

→Model ↓Baselines	Mixtral 8x7B	Mixtral 8x22B	DeepSeekV2 236B	DeepSeekR1 671B
Llama.cpp	328	110	23	6
vLLM	1347	147	97	Fail
DeepSpeed	2621	710	109	Fail
FlexGen*	2199	655	77	Fail
MoE-Lightning*	2237	702	98	Fail
MOE-GEN	2790	907	787	204

Table 7: Prefill throughput (token/s) on C2 with prompt length 512. MOE-GEN outperforms on baselines on larger and more sparse MoE. In prefilling phase MOE-GEN (G) and MOE-GEN (H) has same performance using only GPU.

	16K-8K $B = 50$		8K-16K $B = 50$		8K-4K $B = 100$		4K-2K $B = 200$	
	P	D	P	D	P	D	P	D
vLLM	1182	1	1329	1	1325	1	1359	1
DeepSpeed	2617	1	2621	1	2621	2	2653	3
FlexGen*	2173	2	2187	2	2187	3	2192	5
MoE-Lightning*	2218	2	2221	2	2221	4	2232	6
MOE-GEN (H)	2662	13	2684	13	2686	20	2667	50

Table 8: Throughput for long context generation on C1 with Mixtral-8x7B using Longbench. 16K-8K represents prefill (P) length 16K tokens and decoding (D) length 8K tokens. We conducted preliminary trials with Llama.cpp; however, it proved computationally prohibitive in practice while yielding notably lower performance relative to our other baselines. Consequently, it is omitted from our results.

GEN not significantly outperform DeepSpeed as in Mixtral type of models with less sparsity. MOE-GEN achieves $7.2\times$ more throughput with DeepSeek with higher sparsity.

Batch size in DeepSpeed is bounded by attention peak memory, limiting the batch size to only 8 while DeepSeek-V2 has 160 experts per layer. Thus each expert only has less than 10 tokens to process, leading to GPU computation capability being wasted. FlexGen and MoE-Lightning have the same problem. They can reuse the copied model weights, thus slightly better than DeepSpeed.

Long context performance. We aim to investigate whether MOE-GEN maintains its advantages over baselines under long-context scenarios. As shown in Table 8, for four representative long-context generation tasks, MOE-GEN outperforms the baselines by 7-13×. Although a longer context constrains the maximum batch size that can be cached in host memory, MOE-GEN is designed to maintain a larger intermediate state space for computation, thereby supporting much larger batch sizes than the baselines.

For a prompt length of 512 and a decoding length of 256 for Mixtral-8x7B on C1, the decoding throughput of MOE-GEN is 364 tokens/s. We observe that MOE-GEN’s decoding throughput decreases compared to short-context scenarios. This downgrade arises because, with limited host memory, the largest batch size diminishes as the context length grows. However, the prefill remains stable since a sufficient number

of tokens is provided for the longer context.

5.4. Further Study

We conducted an extensive study of how insufficient batch sizes, CPU attention ratio (ω), and memory constraints affect throughput in MOE-GEN. Our findings demonstrate that with insufficient batch sizes (e.g., 1, 32), MOE-GEN performs better or is comparable with baselines on different models; an optimal ω significantly improve GPU utilization and overall performance. We also demonstrate the influence of the computational power of the CPU on ω . Detailed discussions and additional experiments are provided in the Appendix A.1.

6. Conclusion

MOE-GEN is the first system to enable high-throughput offline inference for large MoE models on a single GPU. Its core innovation, module-based batching, has been extensively evaluated against strong baselines on popular MoE models. MOE-GEN has the potential for broad impact, enabling AI developers to efficiently run offline inference on personal machines and significantly lowering the barrier to adopting large MoE models.

Impact Statement

This paper presents work whose goal is to advance the field of Machine Learning. There are many potential societal consequences of our work, none of which we feel must be specifically highlighted here.

References

- Abdin, M. I., Jacobs, S. A., Awan, A. A., Aneja, J., Awadallah, A., Awadalla, H., Bach, N., Bahree, A., Bakhtiari, A., Behl, H. S., Benhaim, A., Bilenko, M., Bjorck, J., Bubeck, S., Cai, M., Mendes, C. C. T., Chen, W., Chaudhary, V., Chopra, P., Giorno, A. D., de Rosa, G., Dixon, M., Eldan, R., Iter, D., Garg, A., Goswami, A., Gunasekar, S., Haider, E., Hao, J., Hewett, R. J., Huynh, J., Javaheripi, M., Jin, X., Kauffmann, P., Karampatziakis, N., Kim, D., Khademi, M., Kurilenko, L., Lee, J. R., Lee, Y. T., Li, Y., Liang, C., Liu, W., Lin, E., Lin, Z., Madan, P., Mitra, A., Modi, H., Nguyen, A., Norick, B., Patra, B., Perez-Becker, D., Portet, T., Pryzant, R., Qin, H., Radmilac, M., Rosset, C., Roy, S., Ruwase, O., Saarikivi, O., Saied, A., Salim, A., Santacroce, M., Shah, S., Shang, N., Sharma, H., Song, X., Tanaka, M., Wang, X., Ward, R., Wang, G., Witte, P., Wyatt, M., Xu, C., Xu, J., Yadav, S., Yang, F., Yang, Z., Yu, D., Zhang, C., Zhang, C., Zhang, J., Zhang, L. L., Zhang, Y., Zhang, Y., Zhang, Y., and Zhou, X. Phi-3 technical report: A highly capable language model locally on your phone, 2024.
- Aminabadi, R. Y., Rajbhandari, S., Awan, A. A., Li, C., Li, D., Zheng, E., Ruwase, O., Smith, S., Zhang, M., Rasley, J., and He, Y. DeepSpeed-Inference: Enabling efficient inference of transformer models at unprecedented scale. In *SC*, pp. 46:1–46:15. IEEE, 2022.
- Asai, A., Min, S., Zhong, Z., and Chen, D. Retrieval-based language models and applications. In *ACL (tutorial)*, pp. 41–46. Association for Computational Linguistics, 2023.
- Bai, Y., Lv, X., Zhang, J., Lyu, H., Tang, J., Huang, Z., Du, Z., Liu, X., Zeng, A., Hou, L., Dong, Y., Tang, J., and Li, J. LongBench: A bilingual, multitask benchmark for long context understanding. In *ACL (1)*, pp. 3119–3137. Association for Computational Linguistics, 2024.
- Cao, S., Liu, S., Griggs, T., Schafhalter, P., Liu, X., Sheng, Y., Gonzalez, J. E., Zaharia, M., and Stoica, I. MoE-Lightning: High-throughput moe inference on memory-constrained gpus, 2024.
- Chiang, W., Zheng, L., Sheng, Y., Angelopoulos, A. N., Li, T., Li, D., Zhu, B., Zhang, H., Jordan, M. I., Gonzalez, J. E., and Stoica, I. Chatbot arena: An open platform for evaluating llms by human preference. In *ICML. OpenReview.net*, 2024.

- Cobbe, K., Kosaraju, V., Bavarian, M., Chen, M., Jun, H., Kaiser, L., Plappert, M., Tworek, J., Hilton, J., Nakano, R., Hesse, C., and Schulman, J. Training verifiers to solve math word problems, 2021.
- Costa-jussà, M. R., Cross, J., Çelebi, O., Elbayad, M., Heafield, K., Heffernan, K., Kalbassi, E., Lam, J., Licht, D., Maillard, J., Sun, A., Wang, S., Wenzek, G., Youngblood, A., Akula, B., Barrault, L., Gonzalez, G. M., Hansanti, P., Hoffman, J., Jarrett, S., Sadagopan, K. R., Rowe, D., Spruit, S., Tran, C., Andrews, P., Ayan, N. F., Bhosale, S., Edunov, S., Fan, A., Gao, C., Goswami, V., Guzmán, F., Koehn, P., Mourachko, A., Ropers, C., Saleem, S., Schwenk, H., and Wang, J. No language left behind: Scaling human-centered machine translation, 2022.
- Cui, W., Han, Z., Ouyang, L., Wang, Y., Zheng, N., Ma, L., Yang, Y., Yang, F., Xue, J., Qiu, L., Zhou, L., Chen, Q., Tan, H., and Guo, M. Optimizing dynamic neural networks with brainstorm. In *OSDI*, pp. 797–815. USENIX Association, 2023.
- Dao, T. FlashAttention-2: Faster attention with better parallelism and work partitioning. 2024.
- DeepSeek-AI, Liu, A., Feng, B., Wang, B., Wang, B., Liu, B., Zhao, C., Deng, C., Ruan, C., Dai, D., Guo, D., Yang, D., Chen, D., Ji, D., Li, E., Lin, F., Luo, F., Hao, G., Chen, G., Li, G., Zhang, H., Xu, H., Yang, H., Zhang, H., Ding, H., Xin, H., Gao, H., Li, H., Qu, H., Cai, J. L., Liang, J., Guo, J., Ni, J., Li, J., Chen, J., Yuan, J., Qiu, J., Song, J., Dong, K., Gao, K., Guan, K., Wang, L., Zhang, L., Xu, L., Xia, L., Zhao, L., Zhang, L., Li, M., Wang, M., Zhang, M., Zhang, M., Tang, M., Li, M., Tian, N., Huang, P., Wang, P., Zhang, P., Zhu, Q., Chen, Q., Du, Q., Chen, R. J., Jin, R. L., Ge, R., Pan, R., Xu, R., Chen, R., Li, S. S., Lu, S., Zhou, S., Chen, S., Wu, S., Ye, S., Ma, S., Wang, S., Zhou, S., Yu, S., Zhou, S., Zheng, S., Wang, T., Pei, T., Yuan, T., Sun, T., Xiao, W. L., Zeng, W., An, W., Liu, W., Liang, W., Gao, W., Zhang, W., Li, X. Q., Jin, X., Wang, X., Bi, X., Liu, X., Wang, X., Shen, X., Chen, X., Chen, X., Nie, X., and Sun, X. Deepseek-v2: A strong, economical, and efficient mixture-of-experts language model. *CoRR*, abs/2405.04434, 2024.
- Eliseev, A. and Mazur, D. Fast inference of mixture-of-experts language models with offloading, 2023.
- Fu, Y., Jiang, Y., Huang, Y., Nie, P., Lu, Z., Xue, L., He, C., Sit, M.-K., Xue, J., Dong, L., Miao, Z., Zou, K., Ponti, E., and Mai, L. MoE-CAP: Cost-accuracy-performance benchmarking for mixture-of-experts systems, 2024.
- Harma, S. B., Chakraborty, A., Kostenok, E., Mishin, D., Ha, D., Falsafi, B., Jaggi, M., Liu, M., Oh, Y., Subramanian, S., and Yazdanbakhsh, A. Effective interplay between sparsity and quantization: From theory to practice, 2024.
- He, X., Zhang, S., Wang, Y., Yin, H., Zeng, Z., Shi, S., Tang, Z., Chu, X., Tsang, I. W., and Ong, Y. ExpertFlow: Optimized expert activation and token allocation for efficient mixture-of-experts inference, 2024.
- Hendrycks, D., Burns, C., Basart, S., Zou, A., Mazeika, M., Song, D., and Steinhardt, J. Measuring massive multi-task language understanding. In *ICLR*. OpenReview.net, 2021.
- Hwang, R., Wei, J., Cao, S., Hwang, C., Tang, X., Cao, T., and Yang, M. Pre-gated MoE: An algorithm-system co-design for fast and scalable mixture-of-expert inference. In *ISCA*, pp. 1018–1031. IEEE, 2024.
- Jiang, A. Q., Sablayrolles, A., Mensch, A., Bamford, C., Chaplot, D. S., de Las Casas, D., Bressand, F., Lengyel, G., Lample, G., Saulnier, L., Lavaud, L. R., Lachaux, M., Stock, P., Scao, T. L., Lavril, T., Wang, T., Lacroix, T., and Sayed, W. E. Mixtral of experts, 2024a.
- Jiang, X., Zhou, Y., Cao, S., Stoica, I., and Yu, M. NEO: saving GPU memory crisis with CPU offloading for online LLM inference, 2024b.
- Kamahori, K., Gu, Y., Zhu, K., and Kasikci, B. Fiddler: CPU-GPU orchestration for fast inference of mixture-of-experts models, 2024.
- Kwon, W., Li, Z., Zhuang, S., Sheng, Y., Zheng, L., Yu, C. H., Gonzalez, J., Zhang, H., and Stoica, I. Efficient memory management for large language model serving with pagedattention. In *SOSP*, pp. 611–626. ACM, 2023.
- Li, J., Jiang, Y., Zhu, Y., Wang, C., and Xu, H. Accelerating distributed MoE training and inference with Lina. In *USENIX Annual Technical Conference*, pp. 945–959. USENIX Association, 2023.
- Liu, J., Wang, J. H., and Jiang, Y. Janus: A unified distributed training framework for sparse Mixture-of-Experts models. In *SIGCOMM*, pp. 486–498. ACM, 2023.
- Luan, F. S., Mao, Z., Wang, R. Y., Lin, C., Kamsetty, A., Chen, H., Su, C., Veeramani, B., Lee, S., Cho, S., Zinzow, C., Liang, E., Stoica, I., and Wang, S. The streaming batch model for efficient and fault-tolerant heterogeneous execution, 2024.
- Mischler, G., Li, Y. A., Bickel, S., Mehta, A. D., and Mesgarani, N. Contextual feature extraction hierarchies converge in large language models and the brain. *Nature Machine Intelligence*, pp. 1–11, 2024.

- Muennighoff, N., Soldaini, L., Groeneveld, D., Lo, K., Morrison, J., Min, S., Shi, W., Walsh, P., Tafjord, O., Lambert, N., Gu, Y., Arora, S., Bhagia, A., Schwenk, D., Wadden, D., Wettig, A., Hui, B., Dettmers, T., Kiela, D., Farhadi, A., Smith, N. A., Koh, P. W., Singh, A., and Hajishirzi, H. OLMoE: Open mixture-of-experts language models, 2024.
- Narayan, A., Chami, I., Orr, L. J., and Ré, C. Can foundation models wrangle your data? *Proc. VLDB Endow.*, 16(4): 738–746, 2022.
- NVIDIA. TensorRT-LLM. <https://github.com/NVIDIA/TensorRT-LLM>, 2024. Accessed: 2024-05-17.
- NVIDIA. Matrix multiplication background user’s guide. <https://docs.nvidia.com/deeplearning/performance/dl-performance-matrix-multiplication/index.html>, 2025. Accessed: 2025-01-27.
- Ollama. Ollama. <https://github.com/ollama/ollama>, 2025.
- Patel, P., Choukse, E., Zhang, C., Shah, A., Goiri, Í., Maleki, S., and Bianchini, R. Splitwise: Efficient generative LLM inference using phase splitting. In *ISCA*, pp. 118–132. IEEE, 2024.
- Qwen Team. Qwen1.5-moe: Matching 7b model performance with 1/3 activated parameters”, 2024. URL <https://qwenlm.github.io/blog/qwen-moe/>. Accessed: 2024-05-17.
- Sheng, Y., Zheng, L., Yuan, B., Li, Z., Ryabinin, M., Chen, B., Liang, P., Ré, C., Stoica, I., and Zhang, C. FlexGen: High-throughput generative inference of large language models with a single GPU. In *ICML*, volume 202 of *Proceedings of Machine Learning Research*, pp. 31094–31116. PMLR, 2023.
- Song, X., Zhong, Z., and Chen, R. ProMoE: Fast moe-based LLM serving using proactive caching, 2024.
- Song, Y., Mi, Z., Xie, H., and Chen, H. PowerInfer: Fast large language model serving with a consumer-grade GPU, 2023.
- Tang1, P., Liu, J., Hou, X., Pu, Y., Wang, J., Heng, P.-A., Li, C., and Guo, M. Hobbit: A mixed precision expert offloading system for fast MoE inference, 2024.
- van Renen, A., Stoian, M., and Kipf, A. Dataloom: Simplifying data loading with llms. *Proc. VLDB Endow.*, 17(12):4449–4452, 2024.
- Xue, L., Fu, Y., Lu, Z., Mai, L., and Marina, M. K. MoE-Infinity: Activation-aware expert offloading for efficient moe serving, 2024.
- Yi, R., Guo, L., Wei, S., Zhou, A., Wang, S., and Xu, M. EdgeMoE: Fast on-device inference of moe-based large language models, 2023.
- Yu, G., Jeong, J. S., Kim, G., Kim, S., and Chun, B. Orca: A distributed serving system for transformer-based generative models. In *OSDI*, pp. 521–538. USENIX Association, 2022.
- Zhai, M., He, J., Ma, Z., Zong, Z., Zhang, R., and Zhai, J. SmartMoE: Efficiently training sparsely-activated models through combining offline and online parallelization. In *USENIX Annual Technical Conference*, pp. 961–975. USENIX Association, 2023.
- Zhao, Y., Yang, S., Zhu, K., Zheng, L., Kasikci, B., Zhou, Y., Xing, J., and Stoica, I. BlendServe: Optimizing offline inference for auto-regressive large models with resource-aware batching, 2024.
- Zheng, L., Li, Z., Zhang, H., Zhuang, Y., Chen, Z., Huang, Y., Wang, Y., Xu, Y., Zhuo, D., Xing, E. P., Gonzalez, J. E., and Stoica, I. Alpa: Automating inter- and intra-operator parallelism for distributed deep learning. In *OSDI*, pp. 559–578. USENIX Association, 2022.
- Zhong, S., Liang, L., Wang, Y., Wang, R., Huang, R., and Li, M. AdapMoE: Adaptive sensitivity-based expert gating and management for efficient moe inference, 2024.

→Models	DeepSeek-V2-Lite		Mixtral-8x7B	
→Batch Size	1	32	1	32
vLLM	2.1	28	0.5	5
Llama.cpp	0.4	30	0.2	1.1
DeepSpeed	1.3	41	0.4	7.7
FlexGen*	0.9	35	0.3	5.2
MoE-Lightning(p)*	1.0	37	0.4	6.1
MOE-GEN(G)	5.0	35	1.0	33.6

Table 9: Decoding throughput for small batch sizes. Prompt length 512. Decoding length 32.

A. Further Details for Evaluation

A.1. MOE-GEN Further Study

Impact of insufficient batch sizes. The performance gains of MOE-GEN primarily stem from high GPU utilization and enhanced computation-memory overlapping, achievable through large batch sizes. To enable large input batches without running into memory limitations (OOM), we adopt fine-grained memory management techniques alongside design decisions such as full KV-cache offloading, appropriate module buffer sizing, and optimal module micro-batch selection.

These performance advantages diminish as the batch size decreases, which often occurs due to limited host memory capacity. In the extreme scenario of a batch size of one, only a small subset of experts is activated during each forward pass. Since MOE-GEN does not employ heuristics to predict expert activations, it defaults to on-demand fetching after the router stage. Despite this limitation, as shown in Table 9, MOE-GEN still outperforms baselines for models such as Mixtral-8x7B and DeepSeek-V2-Lite at batch size one. This observation indicates that existing baselines deliver lower throughput compared to a strategy relying purely on on-demand copying, partly because they are not specifically optimized for latency-sensitive MoE inference and offloading scenarios.

However, for a batch size of 32, MOE-GEN does not exhibit performance advantages on DeepSeek-V2-Lite. Since the model is relatively small (30GB), a significant portion of the model and its KV-cache can remain persistently in GPU memory under the C1 scenario. Many baselines effectively exploit this capability, whereas MOE-GEN deliberately offloads more data to host memory to free GPU resources, anticipating larger batch sizes. This design choice introduces additional overhead when working with relatively small models and workloads, thus reducing MOE-GEN’s comparative advantage in this specific case.

Impact of CPU attention ratio ω . The proportion of attention computations offloaded from GPU to CPU (ω) directly influences both the volume of KV-cache data that must be copied to GPU memory and the overall execution time of the CPU-GPU hybrid attention mechanism. We

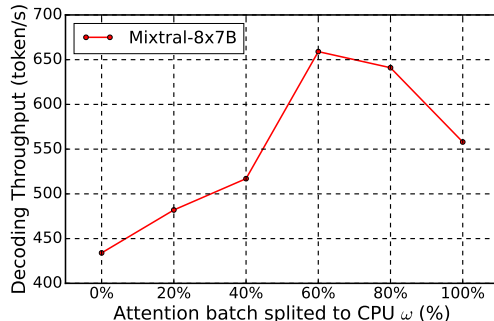


Figure 7: Decoding throughput vs ω . Prompt length 256, decoding length 32. Mixtral 8x7B. C1. Accumulated batch size B 3640.

illustrate this relationship for Mixtral-8x7B under scenario C2 in Figure 7. In this scenario, pure GPU-based inference is memory-bound. Therefore, offloading part of the attention computation to the CPU reduces the amount of KV-cache data copied, alleviating the memory bottleneck. If the CPU kernel’s execution time for attention is shorter than the combined time required to copy the KV-cache to the GPU and process it there, decoding throughput improves because memory-copy overhead is significantly reduced without making the CPU a bottleneck.

Notably, even when the CPU kernel’s runtime slightly exceeds the GPU’s on-demand copy execution time, there can still be throughput benefits, given that memory bandwidth remains the primary limiting factor. However, this advantage holds only up to a certain breakeven point—approximately 60% CPU offloading in our experiments. Beyond this threshold, memory copying ceases to be the critical bottleneck, and further offloading results in GPU idling as it waits for CPU computations, ultimately leading to degraded overall performance.

Influence of CPU computation power. In our offloading setting, when the attention module is memory-bound, utilizing the CPU for attention can improve throughput by (1) reducing stress on HtoD memory bandwidth and (2) leveraging CPU computational resources. The efficiency of the CPU kernel for the attention mechanism ultimately determines whether such improvements are realized. Critical factors include vector width, clock frequency, and the number of CPU cores. If a weaker CPU is used, the time spent on CPU-based attention could exceed that of running attention on the GPU—even after copying the KV-cache—resulting in reduced decoding throughput. In such cases, MOE-GEN would select $\omega = 0$ after the search procedure.

We summarize the attention mechanism workload split ratio under a prompt length of 512 and a decoding length of 256 on Mixtral-8x7B in Table 10, where we simplify the search space for ω to values from 1/10 to 10/10. For C3, the CPU has fewer cores than C1 and C2 limiting its capacity to

CPU:GPU	C1	C2	C3
Mixtral-8x7B	6:4	6:4	3:7
Mixtral-8x22B	N/A	7:3	2:8
DeepSeekV2-236B	N/A	0:10	0:10

Table 10: Attention mechanism workload split ratio. CPU:GPU. Prompt length 512, decoding length 256 on Mixtral-8x7B. C1 cannot hold the model size of Mixtral-8x22B and DeepSeek-V2.

handle the same workload without becoming a performance bottleneck.

B. Further Details for Implementation

MOE-GEN is a throughput-oriented offline inference system designed for single-GPU deployments. Its backend consists of approximately 3,000 lines of C++ and 2,000 lines of Python code. We implement a CPU-based attention kernel utilizing AVX intrinsics. Additionally, MOE-GEN integrates seamlessly with the HuggingFace generation pipeline, currently supporting the greedy decoding strategy

Numerical Consistency of CPU Attention. We implement the widely adopted Grouped Query Attention using the BF16 format with Advanced Vector Extensions (AVX). However, native hardware support for BF16 is limited to relatively recent, high-end CPU generations. To ensure numerical consistency with PyTorch’s GPU attention, we represent BF16 data using FP32, explicitly setting all trailing mantissa bits to zero. All computations and accumulations are performed in FP32 precision. After each dot-product accumulation, the results are rounded according to BF16 rounding rules, and the trailing mantissa bits are reset to zero. This approach ensures numerical consistency comparable to GPU-based attention implementations.

Workload profiling. To effectively support DAG-based scheduling optimization, precise workload profiling is required, specifically, the computational latency and peak memory usage for each module, including the self-attention and expert modules. Latency measurements can be obtained by instrumenting each module’s forward pass with CUDA events, while peak memory usage—including CUDA context, KV cache, and activations—is measured using the torch memory stats related APIs. Additionally, PCIe bandwidth can be profiled throughput using timed cudaMemcpy operations. Before runtime, each module is profiled offline across various batch sizes and sequence lengths, generating comprehensive profiling data.